Environmental Earth Sciences (2020) 79:123
https://doi.org/10.1007/s12665-020-8856-1

ORIGINAL ARTICLE

Hydrochemical analysis and discrimination of mine water source of the Jiaojia gold mine area, China

Ying Wang[1] · Longqing Shi[1] · Min Wang[1] · Tianhao Liu[1]

Received: 23 July 2019 / Accepted: 11 February 2020

Abstract

To study the hydrochemical characteristics of main aquifers in Jiaojia gold mine area and their changing regularities, exploring the main sources of mine water, 244 water samples from the main aquifers and mine water were collected. The principal components were extracted by factor analysis and shows that with the increase of depth, the concentration of Na^+ and Cl^- increased significantly, the water–rock interaction becomes stronger, the water quality develops towards salinization, the total water quality, hydrodynamic conditions, and the connection between groundwater and surface water becomes worse. We extracted the main influential discriminant indexes using principal component analysis (PCA), that is, pH, MH_4^+, NO_3^-, NO_2^-, total hardness, TDS, Fe^{3+}, SO_4^{2-}, Cl^- and F^-. We weighted the extracted discriminant indexes using entropy weight method (EWM), that is in turn, 0.0002, 0.1883, 0.1272, 0.2061, 0.0680, 0.0613, 0.1461, 0.0573, 0.0844, and 0.0613. 55 water samples from each aquifer in the last 5 years were analyzed by hierarchical cluster analysis (HCA), and the relational degree between the main aquifers and mine water was judged by the distance between them; result shows that the main source of mine water is from the hanging wall of fault aquifer, followed by the footwall of fault aquifer. The mine water has little connection with bedrock weathered fractured aquifer, and almost no connection with Quaternary porous aquifer. The PCA–EWM–HCA model established in this paper provides a theoretical basis for identification of mine water inrush source and protection of underground water resources.

Keywords Hydrochemical samples · PCA–EWM–HCA model · Jiaojia fault zone · Water–rock interaction

Introduction

Tanlu fault zone (Fig. 1) is a main fault zone formed in the Mesoproterozoic series of NE trending mega-faults on the East Asian continent, located in the eastern part of China (Tian et al. 2016). It extends more than 2400 km and is 10–200-km wide, and generally 10°–20° northeast trend. The Tanlu fault zone cuts through different geotectonic elements in eastern China; it is the juncture of differential movement of crustal fault blocks, and the deep-source magmatic active zone. Its scale is magnificent, structure is complex and with abundant mineral resources. The ore-controlling structure in Jiaojia gold mine area is a branch fault of Tanlu fault zone, that is, Jiaojia fault zone (Zhang et al. 2017a, b), which is located in the northeast of Tanlu fault zone. The whole Jiaojia fault zone has the characteristics of separation, composite, expansion and compression, its exposed width is different, the widest part can reach 1000 m, and it has a continuous and stable main crack with basic symmetrically zoned tectonite. Jiaojia gold mine area has huge gold resources with great potential for its unique geographical location; Xincheng Gold Mine, Wangershan Gold Mine, Jiaojia Gold Mine and Sizhuang Gold Mine are the most important mines in there.

The groundwater system in Jiaojia gold mine area is composed of many kinds of aquifers, and there are different degrees of hydraulic connections among aquifers. Under the influence of mining, the input, output and system structure of groundwater system in mining area will inevitably change, which will complicate the hydrogeological conditions and cause water inrush accidents (Elham et al. 2016; Qiu et al. 2016). With the increase of mining depth in Jiaojia

✉ Longqing Shi
17863956865@163.com

[1] State Key Laboratory of Mining Disaster Prevention and Control Co-founded by Shandong Province and the Ministry of Science and Technology, Shandong University of Science and Technology, Qingdao 266590, China

Published online: 03 March 2020

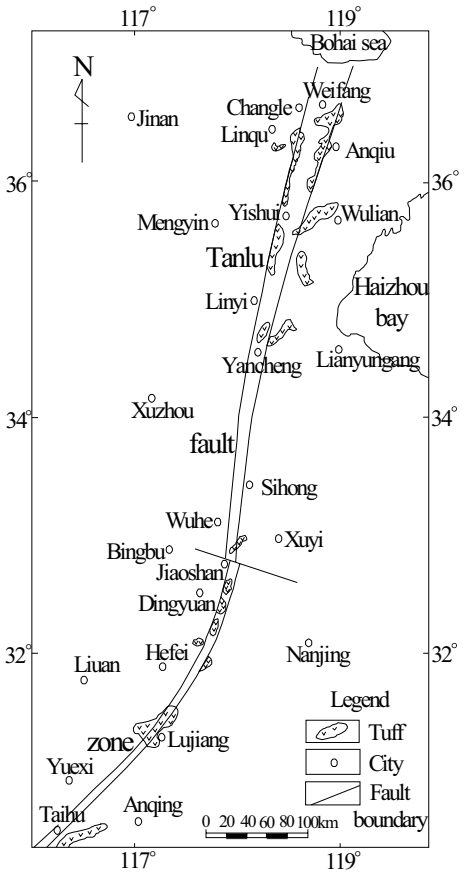

Fig. 1 Tanlu fault zone

gold mine area, the water–rock interaction (WRI) of aquifer is more intense, and the composition of mine water is more complex with unknown source (Huang and Wang 2018a; Xu et al. 2019), which has a certain impact on the further mining of gold mine. In addition, in Jiaojia gold mining area, villages are dense and water wells are widely distributed. Villagers' drinking water, irrigation water and factory water all come from underground water; they mainly come from Quaternary and bedrock weathered fractured aquifers, which have a great impact on residents' lives. Therefore, it is of great significance to study the hydrochemical evolution of main aquifers and exploring the sources of mine water (Jiang et al. 2017; Qian et al. 2018; Sattam et al. 2017).

In order to predict water inrush, for a long time, extract hydrochemical information during lead times of water inrush (Wang and Shi 2019; Huang and Chen 2011; Huang and Wang 2018b; Michael 2007; Wang et al. 2011), comparison of water quality types (Chen et al. 2012; Chidambaram et al. 2013; Shaji et al. 2009), standard component identification (Abhiroop and Kumar 2016; Nordstrom 2011; Tichomirowa et al. 2010; Yang et al. 2016), multiple statistic method (Chen et al. 2017; Giri and Singh 2014; Zhang et al. 2017a, b) are used to identify types of water inrush sources. This kind of achievement only regards the groundwater system of the main aquifers as a simple combination of isolated aquifers, only focus on the static hydrochemical field of a single aquifer, seldom considers the hydrochemical evolution caused by the change of groundwater circulation conditions in the view of time and space, so that the applicability of the water source identification model in the subsequent production process of minerals is limited. In this paper, 244 water samples of Quaternary porous aquifer, bedrock weathered fractured aquifer, the hanging wall of fault aquifer, the footwall of fault aquifer and mine water in Jiaojia gold mine area were collected; the hydrochemical evolution and main water–rock interactions of each aquifer were studied by factor analysis. On the basis of extracted the main influential discriminant indexes by using PCA, EWM is used to weigh the extracted discriminant indexes. 55 water samples from each aquifer in the last 5 years were analyzed by HCA. This model can study not only the source of mine water, but also the relationship and interaction among the main aquifers that affect the source of mine water. It is more intuitive and effective, and provides a theoretical basis for identification of mine water inrush source and protection of underground water resources.

Materials and methods

Study area

Physical geography and stratigraphy

Jiaojia fault zone is located in the middle east part of China (Fig. 2). The study area is high in the southeast and low in the northwest. Wanger Mountain is the highest point with an elevation of 177.5 m. The eastern part of the Jiaojia gold mine area is a hilly region dominated by denudation, the elevation is generally 40–60 m, the slope gradient of topography is large, the valleys are well developed with exposed bedrock; the western part is alluvial–proluvial plain with elevation of 22–35 m, the terrain slopes gently with 6‰, tilting Northwest. The climate in this area belongs to warm temperate continental monsoon climate. Surface water system is not developed, the largest river is Zhuqiao River, followed by the Gonglong River, which has dried up all the year round in recent years.

Jiaojia gold mine area strata are relatively simple, the Cenozoic Quaternary is distributed in northwest area, the Archaean and Proterozoic Jiaodong group (Ar-Ptljf) is distributed in the southwestern part of the study area, the hanging wall of fault zone is mostly covered by Quaternary with widespread magmatic rocks. It developed a continuous main fracture surface marked by gray–black fault gouge and a complete set of fault-rock zones (Fig. 3),

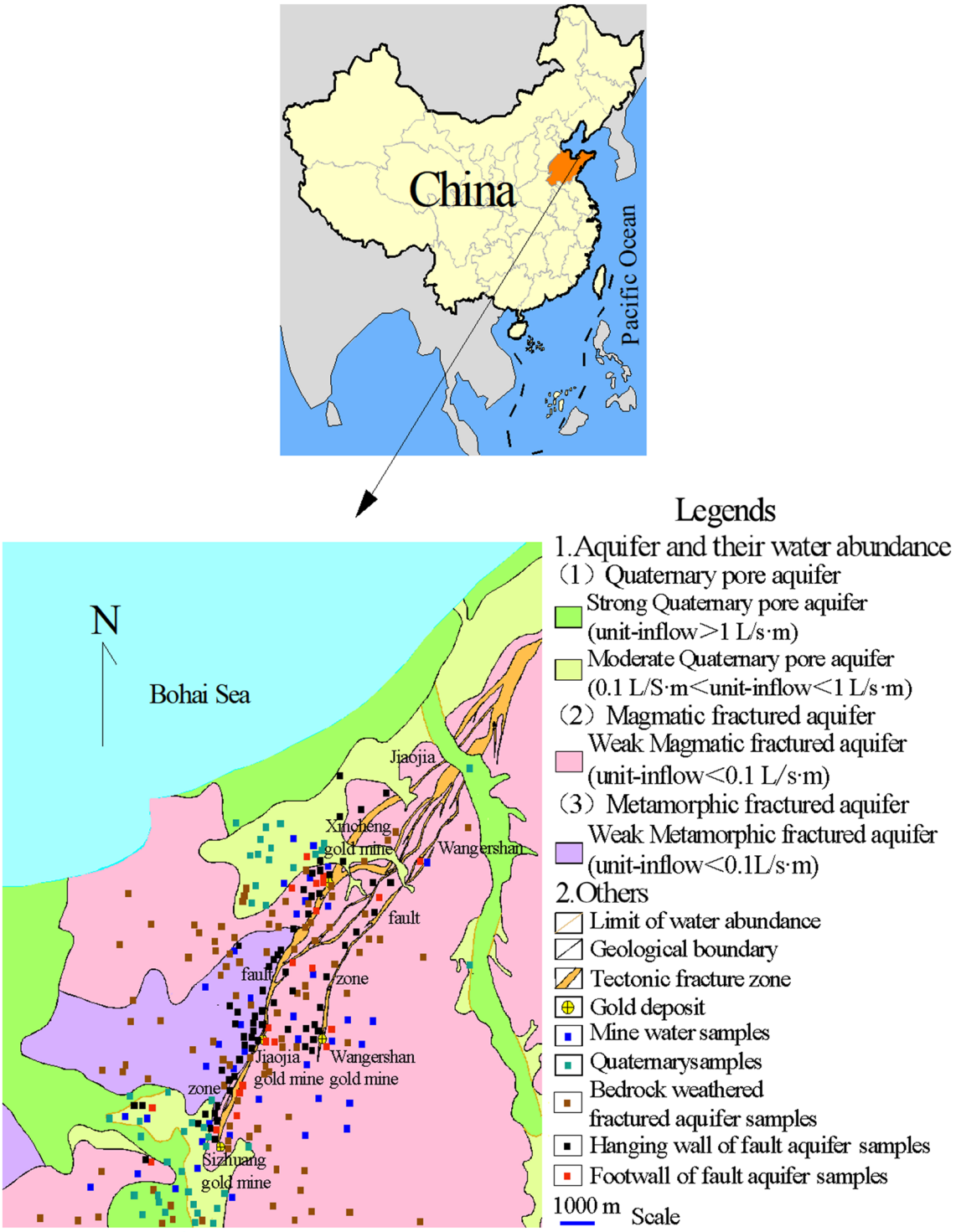

Fig. 2 Geographic location of the Jiaojia gold mine area, its fault distribution, aquifer water-bearing property, and water sampling locations

which are basically symmetrical zoning of tectonites along with the middle of the main fracture surface as the boundary. The hanging wall of fault zone is in turn beresitizatic cataclastic metagabbro, beresitizatic metagabbro, and beresitizatic granite; footwall is in turn beresitizatic cataclastic rock, beresitizatic granitic cataclastic rock, beresitizatic granite, and cataclastic granite. The rock fracture is poorly developed and closed, their permeability is very poor, and they form a water-resisting zone together with the main fracture surface. Ore bodies mainly occur

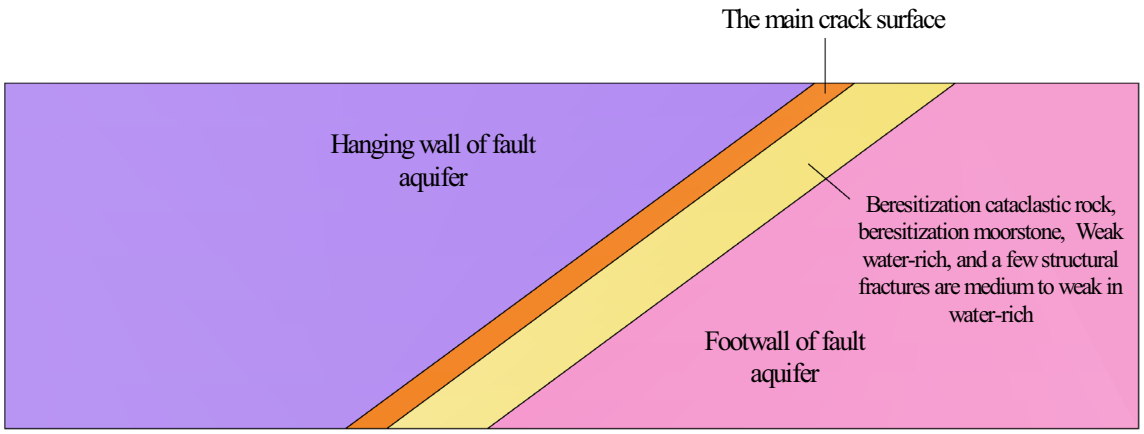

Fig. 3 Fault cross-section diagram

in tectonic altered rocks with high alteration degree under the main fracture surface.

Hydrogeological characteristics of aquifers and confining bed

The main aquifers and confining bed in the Jiaojia gold mine area are Quaternary porous aquifer, bedrock weathered fractured aquifer, hanging wall of fault aquifer, fault gouge, and footwall of fault aquifer (Fig. 4).

Quaternary porous aquifer is mainly distributed along the coast and on both sides of rivers, which are mainly composed of sandy clay, various kinds of sand and gravels with local thin silty clay layer. The Quaternary is dominated by littoral facies, riverbed facies and floodplain facies, with a small amount of piedmont alluvial–diluvial facies deposited locally. In the northwest of Jiaojia gold mine area, there is a small scale of piedmont diluvium with small thickness. The water-bearing property of Quaternary porous aquifers in the west of Jiaojia fault zone, both sides of Zhuqiao and Gunlong river, and coastal plain is from moderate to strong; the permeability coefficient is about 1–15 m/d; the unit-inflow is about 1–4 L/s.m. Most of the Quaternary in hilly areas are dry and anhydrous, the same as the groundwater falling funnel around mining area.

Bedrock weathered fractured aquifer is located under the Quaternary porous aquifer and southern exposed bedrock areas, which is distributed in the entire study area, and composed of metagabbro, phyllic cataclastic rock, phyllic granitic cataclastic rock, phyllic granite, and monzonitic granite with poor to moderate water-bearing property. In addition, the fracture in bedrock weathered fractured aquifer of metagabbro are medium to more developed, and the water-bearing property varies greatly according to the geomorphological location and the water-bearing property of overlying Quaternary, the water-bearing property of bedrock

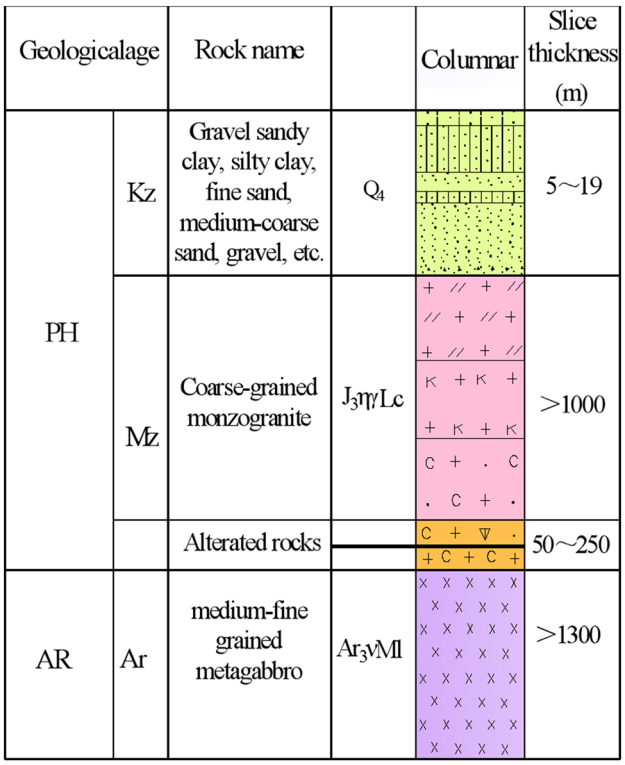

Fig. 4 Comprehensive hydrogeological column of Jiaojia fault zone area

weathered fractured aquifer of metagabbro is mainly moderate with weak water-bearing property in some parts of the area.

Hanging wall of fault aquifers is mainly distributed along the west side of the Jiaojia fault zone and the derived wangershan fault zone, below the bedrock weathered fractured aquifer, which is mainly composed of metagabbro, monzonitic granite, metabagenite cataclastic rock, and

monzonitic granitic cataclastic rock with poor water-bearing property. It is an indirect water-filling aquifer with a thickness of more than 1000 m, but due to the influence of mining engineering, hanging wall of fault aquifer can be transformed into a direct water-filling aquifer of gold deposits. Among them, the fracture of metagabbro is poor to medium developed, some segments are affected by tectonic faults, and the fracture is mostly closed or filled with carbonate. According to the data of borehole pumping test, it can be seen that its water-bearing property is very weak and permeability is poor, the permeability coefficient is about 0.000042–0.0034 m/d, and it can almost be regarded as a confining bed without revealing the NW guide water fracture.

Confining bed composed by fault gouge is located in the middle of Jiaojia fault zone, hard plastic to hard, the thickness is 2–40 cm, the overall trend towards 30°, northwest tendency, the dip angle is 16–40° and the near surface is 60–70° steeper. The main marker is black and gray fault gouge, which is continuously distributed and has well water-resisting property.

The footwall of fault aquifer is mainly distributed along the Jiaojia fault zone at the bottom of the confining bed composed by fault gouge, which is mainly composed of phyllic granitic cataclastic rock, phyllic granite, and granodiorite with poor water-resisting property; it is a direct water-filling aquifer of gold deposits. Among them, the medium-grained monzogranite is mainly distributed in the east part of the Jiaojia fault zone and is mainly composed of medium-grained monzogranite and altered rocks. Rock fractures are medium to more developed, small faults are well developed, and there is no filling or a small amount of kaolin and chlorite filling in the fractures. The permeability and water-bearing property are slightly better than the hanging wall, and the permeability coefficient is about 0.00083–0.00385 m/d, belonging to the poor water-bearing layer.

Sampling and sample preparation

244 samples from Quaternary porous aquifer, bedrock weathered fractured aquifer, the hanging wall of fault aquifer, the footwall of fault aquifer and mine water in Jiaojia gold mine area during the period of mining from January 1968 to December 2016 were collected, of which 42 were from Quaternary, 96 were from bedrock weathered fractured aquifer, 64 were from the hanging wall of fault aquifer, 20 were from the footwall of fault aquifer, and 22 were from the mine water. Conventional ions mainly include $K^+ + Na^+$ (due to the low K^+ content and similar chemical characteristics to Na^+, Na^+ is used instead) (Yin et al. 2017), Ca^{2+}, Mg^{2+}, Cl^-, SO_4^{2-}, HCO_3^-, CO_3^{2-} and TDS.

Analytical procedures

In this paper, Na^+, Ca^{2+}, Mg^{2+}, Cl^-, SO_4^{2-}, HCO_3^-, CO_3^{2-}, NH_4^+, Fe^{3+}, Fe^{2+}, Al^{3+}, F^-, NO_2^-, NO_3^-, total hardness, pH, oxygen consumption, temperature and TDS values were collected as the original discriminant indexs, the index system was established by using PCA to selected indexs and EWM to weighted, which can improve the clarity of the analysis results and is benefit to the judgement of mine water source. HCA is used to determine the source of mine water by index system; in this study, Q-type cluster analysis of SPSS (Statistical Product and Service Solutions) was applied on sample analysis (Fig. 5). SPSS is the earliest statistical analysis software in the world. It was successfully researched and developed by Norman H. Nie, C. Hadlai (Tex) Hull and Dale H. Bent, three graduate students from Stanford University in the United States, in 1968, and SPSS company was founded at the same time. In 2009, International Business Machines Corporation (IBM) acquired SPSS company, and the software was renamed as IBM SPSS statistics.

(1) PCA

The basic principle of PCA is to project sample data from a matrix into a new space. For a matrix, diagonalization is the process of generating eigenroot and eigenvector, and also the process of projecting them on a normal orthogonal basis. We also use SPSS software for this analysis.

The eigenvalues corresponds to the projection length in the direction of the eigenvector; so the larger the eigenvalue, the more information of original data will include in this direction.

(1) Each sample is regarded as a row vector, and the same discriminant indexes of multiple samples are vertical united to form a sample matrix. Suppose there are n hydrochemical samples, each sample contains p discriminant indexes to form a sample matrix of n rows and p columns. Each row represents a sample.

(2) The sample matrix is standardized to eliminate influence of dimension. The standardization formula is as follows:

$$X_i = \frac{(x_i - \min(x_i))}{(\max(x_i) - \min(x_i))},$$

where X_i is the normalized data; x_i is the original data before normalization; $\min(x_i)$ and $\max(x_i)$ are the minimum and maximum values of the original data of water samples. The final standardized sample matrix is: $X = (X_1, X_2, \ldots, X_P)_{n\times p}$.

(3) The covariance matrix is:

$$s_{ij} = \frac{1}{n-1}\sum_k (x_{ki} - \overline{X_i})(x_{ki} - \overline{X_j}),$$

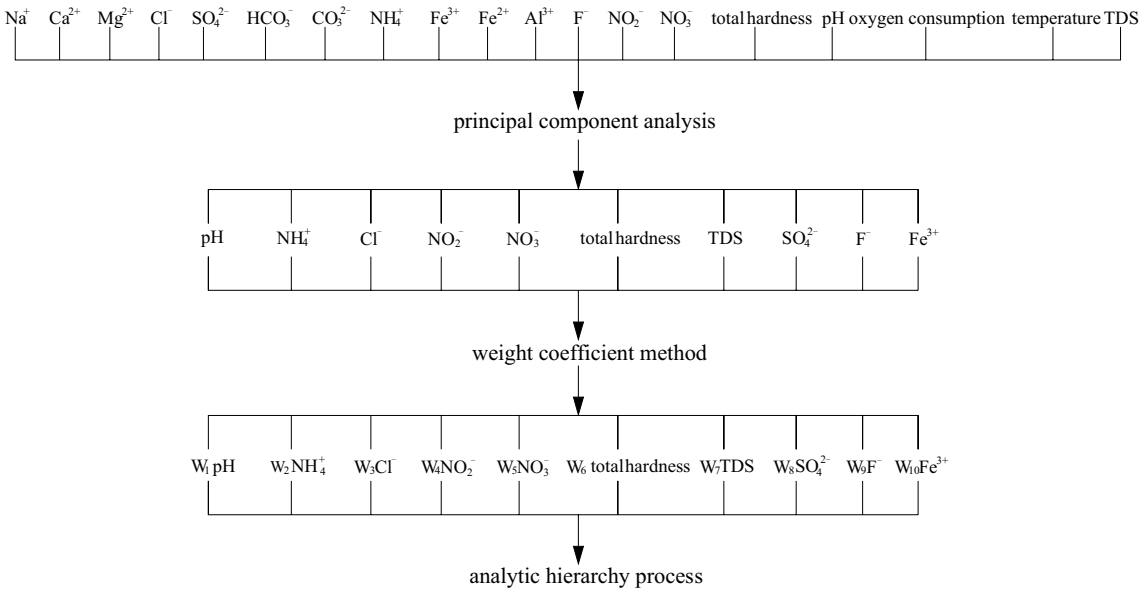

Fig. 5 Technology roadmap of mine water source analysis

where x_{ki} is the element of column i in row k of sample matrix; $\overline{X_i}$ is the average value of column i of sample matrix.

(4) Eigenvalue λ_i and eigenvector ∂_i of covariance matrix $\sum$ were solved by singular value decomposition.

(5) The projection matrix is constructed by eigenvectors to sort eigenvalue λ_i. The projection matrix is constructed by choosing the eigenvectors corresponding to the first k eigenvalues.

$$Y = (\partial_{m1}, \partial_{m2}, \ldots, \partial_{mk})_{p\times k},$$

where ∂_{mk} is the eigenvector corresponding to the eigenvalue λ_k of ranked k.

(6) The projection matrix is used to reduce the dimension of the data, and the contribution rate of each eigenvalue and the principal component load matrix were obtained.

(2) EWM

We use Matlab (matrix and laboratory) software to calculate the entropy weight. Matlab is a commercial mathematical software developed by MathWorks company in the United States, which is used for algorithm development, data visualization, data analysis and numerical calculation. The "entropy" is a measurement to systemic confusion extent, the smaller the information entropy of the index is, the larger the information provided by the index is, the greater the role it plays in the comprehensive evaluation and the higher the weight is. The calculation steps of entropy weight are as follows:

The number of evaluation objects and indexes is determined, and a multi-object multi-index evaluation matrix is created:

$$R = \begin{bmatrix} \gamma'_{11}, & \gamma'_{12}, & \cdots & \gamma'_{1n}, \\ \gamma'_{21}, & \gamma'_{22}, & \cdots & \gamma'_{2n}, \\ \cdots & & \cdots & \\ \gamma'_{m1}, & \gamma'_{m2}, & \cdots & \gamma'_{mn}, \end{bmatrix}.$$

Dimensionless method is applied to the evaluation matrix (R′) according to formula: $\gamma_{ij} = \frac{\gamma'_{ij} - \min(\gamma'_{ij})}{\max(\gamma'_{ij}) - \min(\gamma'_{ij})}$, and obtained the matrix: $R = (\gamma_{ij})_{m\times n}$.

The entropy value of the ith evaluation index is obtained by normalizing matrix R according to formula: $f_{ij} = \frac{\gamma_{ij}}{\sum_{j=1}^{n}\gamma_{ij}} (i = 1, 2, \ldots, n; j = 1, 2, \ldots, m)$,

$$H_i = -\frac{1}{\ln m}\sum_{j=1}^{m} f_{ij} \ln f_{ij};$$

the entropy weight of the ith evaluation index can be expressed as:

$$\omega_i = \frac{1 - H_i}{n - \sum_{i=1}^{n} H_i}.$$

(3) HCA

HCA (Tina et al. 2007) is the taxonomy structure which organizes categories in tree structure according to the certain hierarchical relations, which can automatically classify a set of sample data according to its characteristics and relationship in nature without prior knowledge; it allows samples

with similar characteristics to be clustered together to separate large difference samples. HCA measures the relationship between bodies by various distances. We also use SPSS for cluster analysis. In this paper, euclidean distance between two bodies (x, y) is defined as the square numbers and square root of the difference between the values of k variables of two bodies. It is mathematically defined as:

$$\mathrm{EUCLID}(x, y) = \sqrt{\sum_{i=1}^{k} (x_i - y_i)^2},$$

where x_i is the variable value of the ith variable of x.

Statistical analyses

Based on the 244 hydrochemical samples collected, we used the aqqa software to draw the piper diagram; aqqa is a water conservancy data analysis software written by water chemists, which can provide the function of excellent image display and powerful data analysis. The analysis process is as follows; it can be seen that with the development of gold mining, the hydrochemical type of groundwater and the contents of conventional ions have changed.

In Quaternary porous aquifer (Fig. 6), the concentration of Na^+, Cl^- decreased slightly, Ca^{2+} and Mg^{2+} increased, HCO^{3-} decreased significantly, $SO_4{}^{2-}$ increased significantly, and the hydrochemical type gradually changed from Cl–Na·Ca to $HCO_3{\cdot}SO_4{\cdot}$Cl–Ca. TDS is less than 1.5 g/L before and after mining, the water quality of which is good.

In bedrock weathered fractured aquifer (Fig. 7), the concentration of Na^+, $SO_4{}^{2-}$ and HCO_3 decreased, Ca^{2+} increased, Mg^{2+} decreased slightly, Cl^- increased significantly, and the hydrochemical type gradually changed from HCO_3–Ca to $HCO_3{\cdot}SO_4{\cdot}$Cl–Ca. The increased TDS is mostly less than 1.5 g/L, a few of them are from 1.5 to 10 g/L, and the water quality is less well.

In hanging wall of fault aquifer (Fig. 8), the concentration of Na^+ decreased, Ca^{2+}, $SO_4{}^{2-}$ and $HCO_3{}^-$ increased, and the hydrochemical type gradually changed from $HCO_3{\cdot}$Cl–Na·Ca to $HCO_3{\cdot}SO_4{\cdot}$Cl–Ca. The decreased TDS is mostly less than 1.5 g/L, a few of them are from 1.5 to 10 g/L, and the water quality is less well.

In footwall of fault aquifer (Fig. 9), the concentration of Na^+ and HCO_3 decreased, Ca^{2+} increased, Cl^- increased significantly, and the hydrochemical type gradually changed from $HCO_3{\cdot}$Cl–Ca to $HCO_3{\cdot}SO_4{\cdot}$Cl–Ca. The decreased TDS is mostly from 1.5 to 10 g/L, the water quality of which is bad.

In mine water (Fig. 10), the concentration of Na^+ increased, Ca^{2+} decreased significantly, Cl^- increased significantly, $HCO_3{}^-$ decreased, and the hydrochemical type gradually changed from HCO_3–Ca to Cl–Na. The decrease TDS is mostly less than 1.5 g/L, and a few of them are from 1.5 to 10 g/L, which the water quality is less well in general.

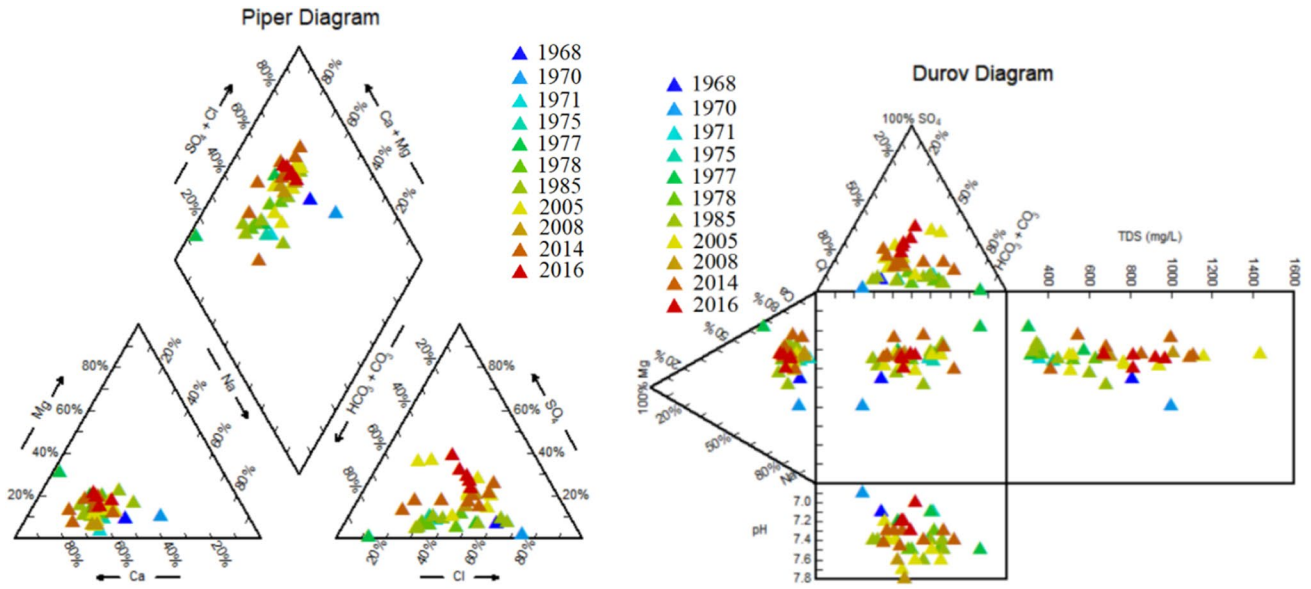

Fig. 6 Piper diagram of Quaternary pore aquifer

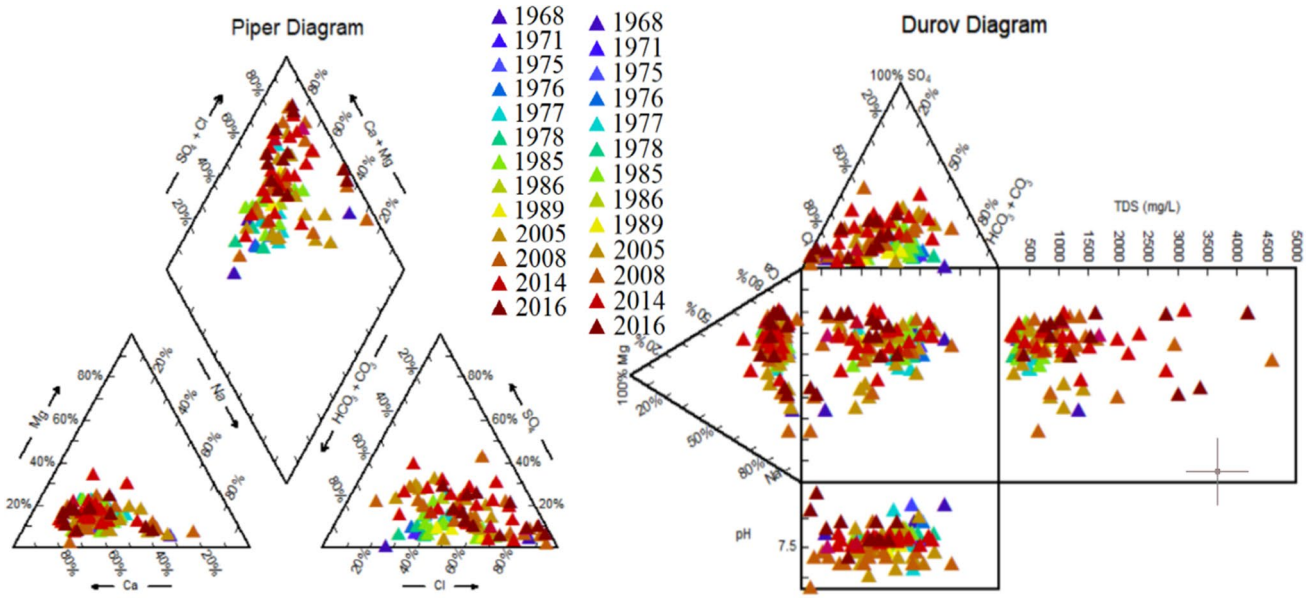

Fig. 7 Piper diagram of bedrock weathered fractured aquifer

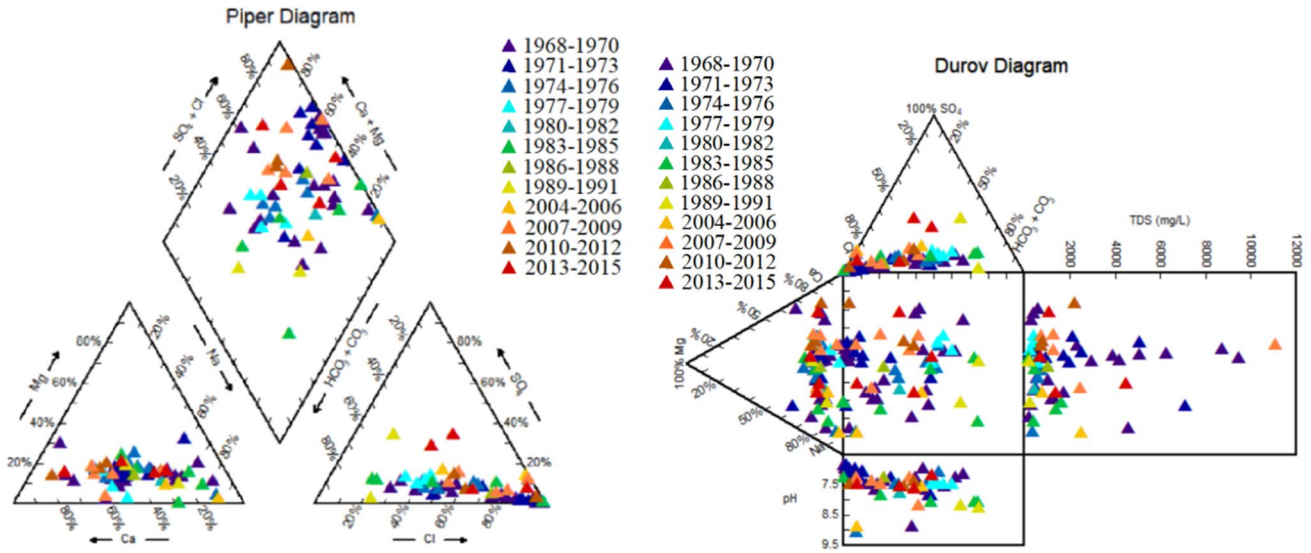

Fig. 8 Piper diagram of the hanging wall of fault aquifer

Results and discussion

Water–rock interaction of main aquifers

Factor analysis is based on PCA. After rotation, principal components factors were obtained. In the rotation factor loading figure (Fig. 11) of Quaternary porous aquifer, SO_4^{2-}, Ca^{2+} and Mg^{2+} have high load values on the axis of principal component 1, with percentages of 91.9%, 76.7% and 75.1%, respectively. The high load of Ca^{2+} and Mg^{2+} is related to the dissolution of gypsum and carbonate rocks. The high load of SO_4^{2-} is caused by the dissolution of gypsum and other sulfate-bearing minerals. According to the data, the strata in the Jiaojia gold mine area contain different amounts of sulphur ore, iron ore and marble; mining activities are conducive to the occurrence of oxidation. When there is carbonate or sulphate in the underground strata, this kind of acid groundwater will accelerate the dissolution of carbonate or sulphate minerals. As a result, the pH increases and the load values of SO_4^{2-}, Ca^{2+} and Mg^{2+} are higher. The relevant chemical reaction equations are as follows:

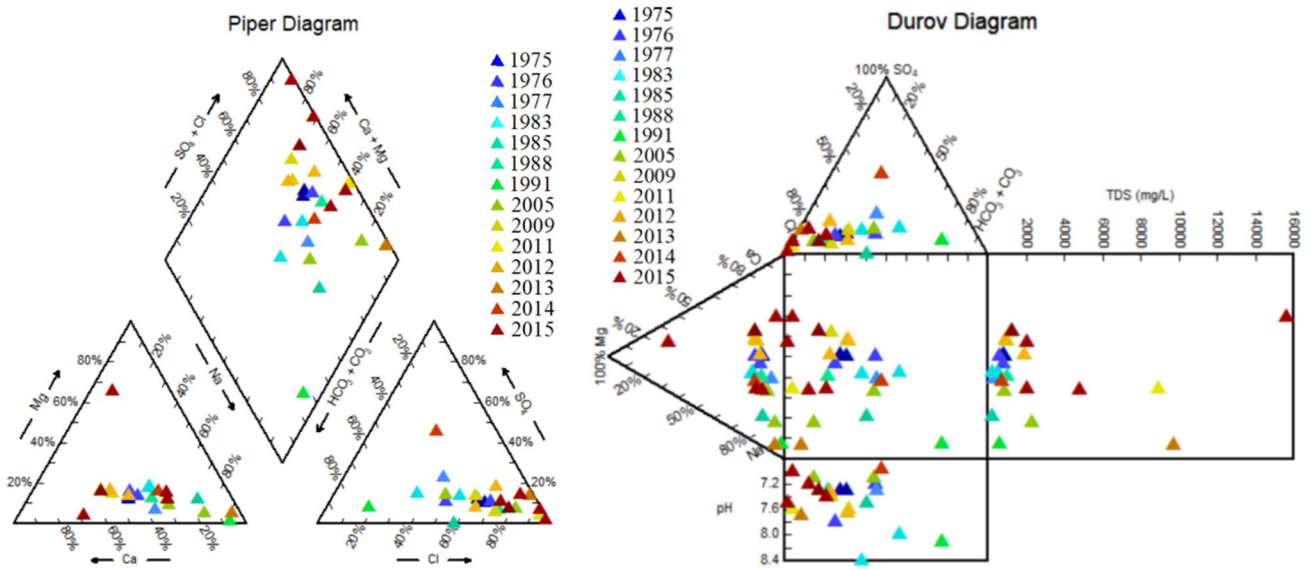

Fig. 9 Piper diagram of footwall of fault aquifer

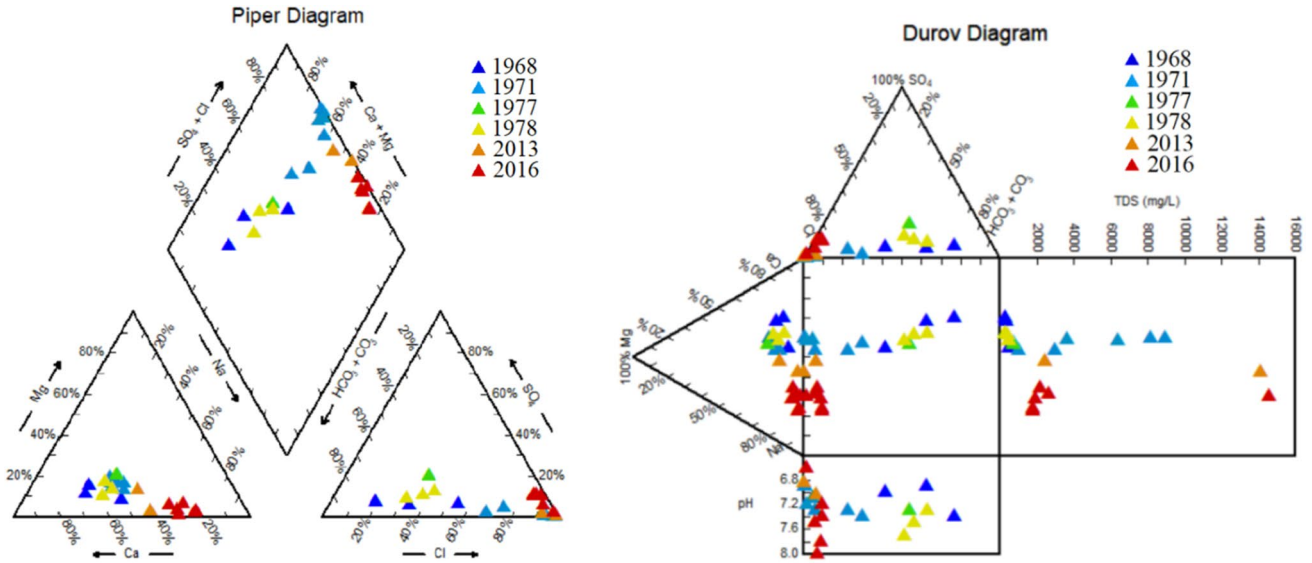

Fig. 10 The piper diagram of mine water

$$FeS_2^+ 15/4O_2 + 7/2H_2O \rightarrow Fe(OH)_3 \downarrow + 2SO_4^{2-} + 4H^+,$$

$$CaCO_3 + H^+ \rightarrow Ca^{2+} + HCO_3^-,$$

$$CaMg(CO_3)_2 + 2H^+ \rightarrow Ca^{2+} + Mg^{2+} + 2HCO_3^-,$$

$$CaSO_4 \rightarrow Ca^{2+} + SO_4^{2-},$$

$$MgSO_4 \rightarrow Mg^{2+} + SO_4^{2-}.$$

HCO_3^-, Na^+ and Cl^- have high load values on the axis of principal component 2, with percentages of 73.8%, 77.2% and 81.5%, respectively. The high load of HCO_3^- indicates that groundwater has a certain relationship with atmospheric precipitation and surface water, and the groundwater dynamic condition is better. The similar loads of Na^+ and Cl^- indicate that groundwater has undergone leaching. The high load of Na^+ is due to the cation exchange reaction between Na^+ and Ca^{2+}, Mg^{2+} when the groundwater containing Ca^{2+} and Mg^{2+} flow through the rock strata where Na^+ is mainly adsorbed, which increases the concentration of Na^+, and decreases Ca^{2+} and Mg^{2+} in groundwater. The relevant chemical reaction equations are as follows:

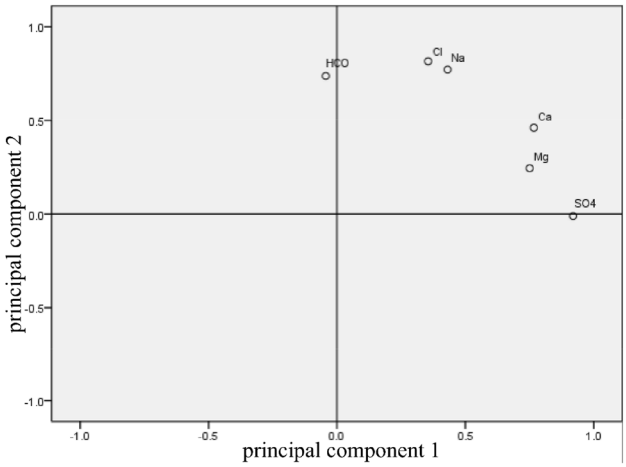

Fig. 11 Factor loading distribution of Quaternary aquifer

$$2Na^{+}(rock) + Ca^{2+}(water) \rightarrow 2Na^{+}(water) + Ca^{2+}(rock),$$

$$2Na^{+}(rock) + Mg^{2+}(water) \rightarrow 2Na^{+}(water) + Mg^{2+}(rock).$$

In the rotation factor loading figure (Fig. 12) of bedrock weathered fractured aquifer, Na^{+} and Cl^{-} have high load values on the axis of principal component 1, with percentages of 87.7% and 97.5%, respectively, and the load value of Cl^{-} is slightly higher than Na^{+}, which indicates that the ion exchange between Na^{+} and Ca^{2+} is strong. HCO_3^{-} has a high load value on the axis of principal component 2, with percentages of 93.4%, which indicates that groundwater is related to atmospheric precipitation and surface water, and the groundwater dynamic condition is better.

In the rotation factor loading figure (Fig. 13) of hanging wall of fault aquifer, HCO_3^{-} has very low load value on the axis of the two principal components, with percentages of − 68.8% and 15.9%, respectively, which indicates that there is almost no connection between the hanging wall of fault aquifer and the atmospheric precipitation, shallow underground water. With the increase of the depth, the hydrodynamic conditions become worse and the water–rock interaction is intense. Na^{+}, Cl^{-}, Ca^{2+}, Mg^{2+} have very high load values on the axis of principal component 1, with percentages of 76.6%, 90.5%, 79.3% and 75.1%, respectively, which indicates that the cation exchange reaction between Na^{+} and Ca^{2+}, Mg^{2+} is strong. In addition, SO_4^{2-} has a high load value on the axis of principal component 2, with percentages of 94.2%, which is related to the dissolution of gypsum and other sulfate minerals.

In the rotation factor loading figure (Fig. 14) of footwall of fault aquifer, HCO_3^{-} has almost no load value on the axis of the two principal components, with percentages of 1.8%, and − 91.0%, respectively, which indicates that there is no connection between the footwall of fault aquifer and the shallow underground water, the water–rock interaction is intense, and the development of water quality towards salinization. SO_4^{2-}, Na^{+} and Cl^{-} have high load values on the axis of principal component 1, with percentages of 94.2%, 90.7%, and 93.6%, respectively. TDS increases, which indicates that may be a certain relationship with seawater, and the characteristics of marine sedimentary water are obvious, the cation exchange reaction is strong. The concentration of Na^{+} increases due to rock dissolution or acidification. In addition, the increase of SO_4^{2-} is related to the dissolution of gypsum and other sulfate minerals.

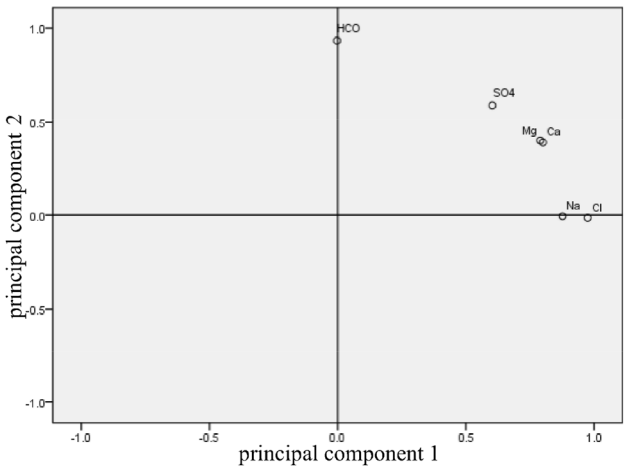

Fig. 12 Factor loading distribution of bedrock weathered fractured aquifer

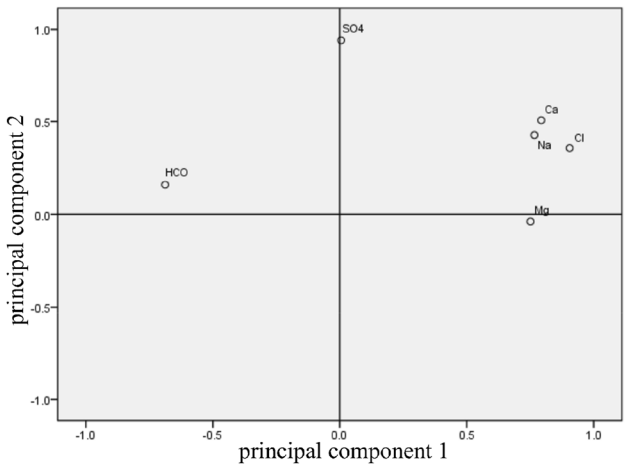

Fig. 13 Factor loading distribution of hanging wall of fault aquifer

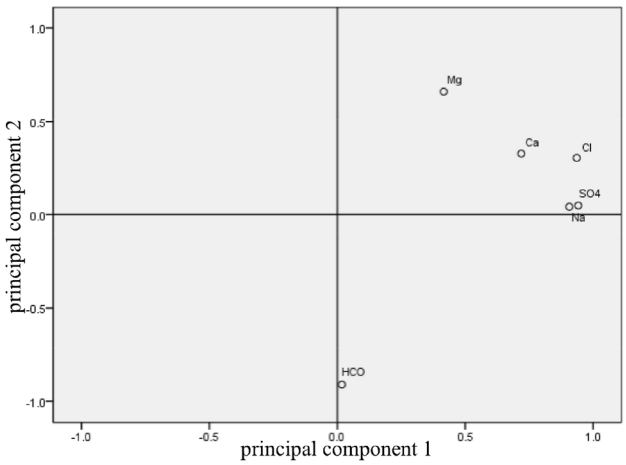

Fig. 14 Factor loading distribution of footwall of fault aquifer

Discrimination of mine water source

The original index of water quality evaluation includes K^+ and Na^+ (due to the low K^+ content and similar chemical characteristics to Na^+, Na^+ is used instead) (Yin et al. 2017), Ca^{2+}, Mg^{2+}, Cl^-, SO_4^{2-}, HCO_3^-, CO_3^{2-}, NH_4^+, Fe^{3+}, Fe^{2+}, Al^{3+}, F^-, NO_2^-, NO_3^-, total hardness, pH, oxygen consumption (mg/L), temperature and TDS. Then the PCA method was used to reduce dimension; it can be seen from the Table 1 that TDS is the heaviest and Fe^{2+} is the lightest in the component load. The first ten discriminant indexes with heavier loads were selected as the main discriminant indexes, that is, TDS, Cl^-, total hardness, NO_2^-, NH_4^+, Fe^{3+}, NO_3^-, SO_4^{2-}, pH and F^-.

The 10 indexes obtained by PCA were weighted according to EWM, and the weights of the main discriminant indexes are W_i ($i = 1, 2, \ldots, 10$) (Table 2). In this paper, the entropy weights were calculated using the Entropy Weight function of MATLAB software.

55 water samples from each aquifer in the last 5 years were selected, multiplied by their respective weights and

Table 1 Principal component load matrix

	Components						
	1	2	3	4	5	6	7
TDS	.956	− .090	− .029	.006	.050	− .004	.035
Cl^-	.951	− .153	− .130	.045	.033	− .069	− .052
Total hardness	.910	− .199	.093	− .002	.169	− .074	.056
NO_2^-	.866	.040	− .123	.130	− .041	− .078	− .174
NH^{4+}	.730	− .200	− .118	− .112	− .023	.145	.268
Fe^{3+}	.691	.175	.467	.185	.199	− .132	− .083
NO_3^-	.104	.641	− .321	− .373	.226	.077	− .065
SO_4^{2-}	.095	.608	− .302	− .333	.247	.158	− .130
pH	.369	.495	− .099	.081	− .400	− .071	.251
F	.192	.420	− .269	− .259	.165	− .306	.146
Ca^{2+}	.034	.133	.657	− .082	.266	.343	.184
Na^+	− .333	.361	.535	− .183	− .080	− .013	.027
Mg^{2+}	.431	.426	.491	.161	.111	− .128	− .063
Oxygen consumption	− .118	.080	− .306	.677	.427	.065	.116
HCO_3^-	− .350	.307	− .139	.642	.253	.078	.166
CO_3^{2-}	.103	.318	− .010	.222	− .564	− .212	.393
Al^{3+}	.228	.319	.003	.162	− .274	.611	.051
Temperature	.385	− .132	− .141	− .024	− .167	.549	− .129
Fe^{2+}	.032	.284	.025	.315	− .286	− .077	− .740

Table 2 Entropy values and weights of EWM

	pH	MH_4^+	NO_3^-	NO_2^-	Total hardness	TDS	Fe^{3+}	SO_4^{2-}	Cl^-	F^-
H_i	0.9997	0.5706	0.7099	0.5301	0.8448	0.8603	0.6668	0.8694	0.8076	0.8603
W_i ($i = 1, 2, \ldots, 10$)	0.0002	0.1883	0.1272	0.2061	0.0680	0.0613	0.1461	0.0573	0.0844	0.0613

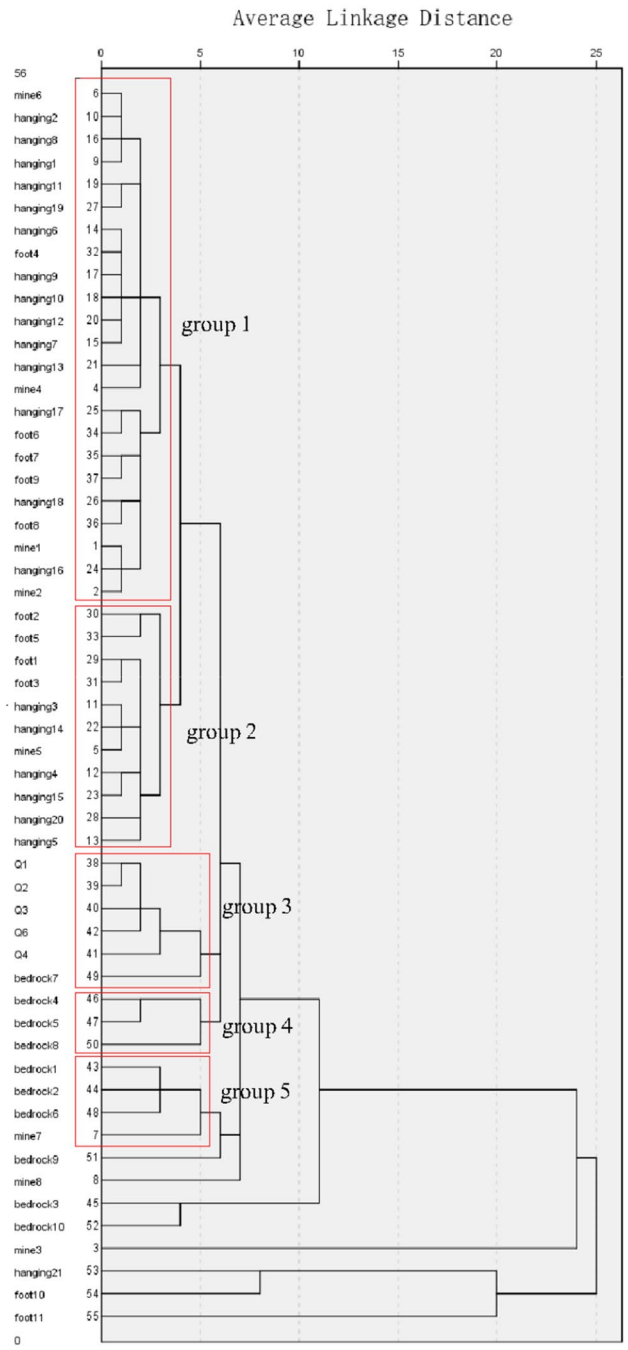

Fig. 15 Dendrogram generated from HCA of water chemistry data

normalized as the original data of HCA, that the results are as follows (Fig. 15): *Q* is Quaternary porous aquifer, bedrock is bedrock weathered fractured aquifer, hanging is the hanging wall of fault aquifer, foot is the footwall of fault aquifer and mine is the mine water.

It can be seen from the upper diagram that the last eight samples were excluded as they are far away from other water samples.

According to groups 1 and 2, 14 water samples from the hanging wall of fault aquifer and 5 water samples from the footwall of fault aquifer are relatively close to the 4 mine water samples, of which hanging 1, 2, 8 and mine 6, hanging 16 and mine 2, hanging 6, 9, 10, 12, 7 and foot 4 are the closest. 6 water samples from the hanging wall of fault aquifer and 4 water samples from the footwall of fault aquifer are relatively close to the 1 mine water sample, of which hanging 3, 14 and mine 5 are the closest. It shows that there is a close hydraulic connection between hanging wall of fault aquifer and the footwall of fault aquifer; the hanging wall of fault aquifer connects closely with the mine water, and the footwall of fault aquifer is second with it.

According to group 3, 5 water samples from Quaternary porous aquifer are relatively close to the 1 water samples from bedrock weathered fractured aquifer. It shows that there is a close hydraulic connection between Quaternary porous aquifer and bedrock weathered fractured aquifer. However, there is no mine water sample in this group, indicating that the Quaternary porous aquifer and bedrock fractured aquifer have little connection with mine water.

According to group 5, 3 water samples from bedrock weathered fractured aquifer are relatively close to the 1 water samples from mine water. It shows that there is some connection between bedrock weathered fractured aquifer and mine water.

In summary, the main source of mine water is from the hanging wall of fault aquifer, followed by the footwall of fault aquifer. The mine water has little connection with bedrock weathered fractured aquifer, and almost no connection with Quaternary porous aquifer. Considering that the gold mining has destroyed the confining bed composed by fault gouge, the water in the hanging wall of fault aquifer flows into the mine through the fractures near the fault zone due to gravity, and forms close hydraulic connection with the footwall of fault aquifer. In addition, for the large thickness of the hanging wall of fault aquifer, it is very difficult for the water of bedrock weathered fractured aquifer and Quaternary porous aquifer to flow into the mine. This result has a significant guiding for the prediction of the source of mine water inrush.

Conclusion

In this paper, based on 244 collected hydrochemical samples, the principal components were extracted by factor analysis and given an interpretative name to study the main WRI under mining effect. 55 water samples from each aquifer in the last 5 years were analyzed by HCA, and the relational degree between the main aquifers and mine water was judged by the distance between them to determine the source of water inrush. The main conclusions are as follows:

(1) With the increase of depth, the concentration of Na^+ and Cl^- increased significantly, the water–rock interaction becomes stronger; the water quality develops towards salinization, and the total water quality becomes worse; the hydrodynamic conditions become worse; and the connection between groundwater and surface water becomes worse. The hanging wall of fault aquifer has a certain relationship with the sea water, the characteristics of marine sedimentary water are obvious, and the cation exchange reaction is strong.
(2) The main influence indexes were selected using PCA, that is, pH, NH_4^+, Cl^-, NO_3^-, NO_2^-, total hardness, TDS, Fe^{3+}, SO_4^{2-}, Cl^- and F^-. The 10 indexes obtained by PCA are weighted according to EWM, and the weights of them are 0.0002, 0.1883, 0.1272, 0.2061, 0.0680, 0.0613, 0.1461, 0.0573, 0.0844 and 0.0613.
(3) The main source of mine water is from the hanging wall of fault aquifer, followed by the footwall of fault aquifer. The mine water has little connection with bedrock weathered fractured aquifer, and almost no connection with Quaternary porous aquifer.

Acknowledgements We gratefully acknowledge the financial support of the National Natural Science Foundation of China (Nos. 41572244, 51804184 and 41807283), the Scientific Research Foundation of Shandong University of Science and Technology for Recruited Talents (2017RCJJ033), the Open Fund Research Project of State Key Laboratory of Mining Disaster Prevention and Control Co-founded by Shandong Province and the Ministry of Science and Technology (MDPC2017ZR05), and Taishan Scholars' Special Funds for Construction Projects. No conflict of interests regarding the publication of this manuscript.

References

Abhiroop C, Kumar MS (2016) Identifying the source and accessing the spatial variations, contamination status, conservation threats of heavy metal pollution in the river waters of Sunderban biosphere reserve, India. J Coast Conserv 20(3):257–269

Chen H, Teng Y, Wang J, Song L (2012) Source apportionment of water pollution in the Jinjiang river (China) using factor analysis with nonnegative constraints and support vector machines. Environ Forensics 13(2):175–184

Chen M, Wu Y, Gao D, Chang M (2017) Identification of coal mine water-bursting source using multivariate statistical analysis and tracing test. Arab J Geosci 10(2):28

Chidambaram S, Anandhan P, Prasanna MV, Srinivasamoorthy K, Vasanthavigar M (2013) Major ion chemistry and identification of hydrogeochemical processes controlling groundwater in and around Neyveli Lignite Mines, Tamil Nadu, South India. Arab J Geosci 6(9):3451–3467

Elham F, Asghar AM, Frank T-CT, Gokmen T (2016) Analysis and assessment of hydrochemical characteristics of maraghehbonab plain aquifer, northwest of Iran. Water Resour Manag 31(3):765–780

Giri S, Singh AK (2014) Risk assessment, statistical source identification and seasonal fluctuation of dissolved metals in the Subarnarekha river, India (Article). J Hazard Mater 265(2014):305–314

Huang P, Chen J (2011) The chemical features of ground water and FDA model used to distinguish source of water burst in Jiaozuo mine area. Coal Geol Explor 39(2):42–46 **(in Chinese)**

Huang P, Wang X (2018a) Groundwater mixing mechanism in multi-aquifer system based on isotopic tracing theory-a case study in the coal mine district, China. Geofluids 2018:1–10

Huang P, Wang X (2018b) Piper-PCA-Fisher recognition model of water inrush source: a case study of the Jiaozuo mining area. Geofluids 2018:1–10

Jiang X, Xiong Z, Liu H, Liu G, Liu W (2017) Distribution, source identification, and ecological risk assessment of heavy metals in wetland soils of a river–reservoir system. Environ Sci Pollut Res 24(1):436–444

Michael R (2007) Giant mine: identification of inflow water types and preliminary geochemical monitoring during reflooding. Mine Water Environ 26(2):102–109

Nordstrom DK (2011) Hydrogeochemical processes governing the origin, transport and fate of major and trace elements from mine wastes and mineralized rock to surface waters. Appl Geochem 26(2011):1777–1791

Qian J, Tong Y, Ma L, Zhao W, Zhang R, He X (2018) Hydrochemical characteristics and groundwater source identification of a multiple aquifer system in a coal mine. Mine Water Environ 37(3):528–540

Qiu M, Shi L, Teng C, Zhou Y (2016) Assessment of water inrush risk using the fuzzy delphi analytic hierarchy process and grey relational analysis in the Liangzhuang coal mine, China. Mine Water Environ 36(1):39–50

Sattam A, Hussain A, Abdullah A-A, Mohamed F, Elkhedr I, Kamal A, Mohammed S, Faisal Z (2017) Hydrochemical characteristics and evaluation of the granite aquifer in the Alwadeen area, southwest Saudi Arabia. Arab J Geosci 10(6):139

Shaji E, Vinayachandran N, Thambi DS (2009) Hydrogeochemical characteristics of groundwater in coastal phreatic aquifers of Alleppey district, Kerala. J Geol Soc India 74(5):585–590

Tian HS, Van Loon AJ, Wang HL (2016) Seismites in the Dasheng Group: new evidence of strong tectonic and earthquake activities of the Tanlu Fault Zone. Sci China Earth Sci 59(3):601–618

Tichomirowa M, Heidel C, Junghans M, Haubrich F, Matschullat J (2010) Sulfate and strontium water source identification by O, S and Sr isotopes and their temporal changes (1997–2008) in the region of Freiberg, central-eastern Germany. Chem Geol 276(2010):104–118

Tina H, Niels OJ, Bruce B-Y (2007) Investigation of hydrochemical characteristics of groundwater from the Cretaceous-Eocene limestone aquifer in southern Ghana and southern Togo using hierarchical cluster analysis. Hydrogeol J 15(5):977–989

Wang D, Shi L (2019) Source identification of mine water inrush: a discussion on the application of hydrochemical method. Arab J Geosci 12(2):12–58

Wang X, Xu T, Huang D (2011) Application of distance discriminance in identifying water inrush resource in similar coalmine. J China Coal Soc 36(8):1354–1358 **(in Chinese)**

Xu D, Shi L, Qu X, Tian J, Wang K, Liu J (2019) Leaching behavior of heavy metals from the coal gangue under the impact of site ordovician limestone karst water from closed shandong coal mines, North China. Energy Fuels 33(10):10016–10028

Yang Q, Wang L, Ma H, Yu K, Martín JD (2016) Hydrochemical characterization and pollution sources identification of groundwater in Salawusu aquifer system of Ordos Basin, China. Environ Pollut 216:340–349

Yin XX, Chen LW, Xie WP, Xu DQ, Zeng W, Liu YX (2017) Main water-rock interactions and hydrochemical evolution in the aquifers under the mining-induced disturbance in a mining district. Hydrogeol Eng Geol 44(5):33–39

Zhang H, Jiang Y, Wang M, Wang P (2017a) Spatial assessment and source identification of heavy metals pollution in surface water using several chemometric techniques. Environ Sci Pollut Res 24(3):2890–2903

Zhang K, Lu Q, Yan J, Hu H, Fu G (2017b) The electrical resistivity signature of a fault controlling gold mineralization and the implications for Mesozoic mineralization: a case study from the Jiaojia Fault, eastern China. Acta Geophys 65(4):727–741